Applied Catalysis B: Environmental 115–116 (2012) 81–89

Contents lists available at SciVerse ScienceDirect

Applied Catalysis B: Environmental

journal homepage: www.elsevier.com/locate/apcatb

One-step, hydrothermal synthesis of nitrogen, carbon co-doped titanium dioxide (N,C—TiO_2) photocatalysts. Effect of alcohol degree and chain length as carbon dopant precursors on photocatalytic activity and catalyst deactivation

D. Dolat[a], N. Quici[b], E. Kusiak-Nejman[a], A.W. Morawski[a], G. Li Puma[b,*]

[a] West Pomeranian University of Technology, Szczecin, Institute of Chemical and Environmental Engineering, Pułaskiego 10, 70-322 Szczecin, Poland
[b] Photocatalysis and Photoreaction Engineering, Department of Chemical Engineering, Loughborough University, Loughborough, LE11 3TU, United Kingdom

ARTICLE INFO

Article history:
Received 30 October 2011
Received in revised form
30 November 2011
Accepted 3 December 2011
Available online 9 December 2011

Keywords:
Photocatalysis
TiO_2
Degradation
Nitrogen/carbon co-modification
Catalyst lifetime
Intrinsic photocatalytic activity
Volumetric rate of photon absorption

ABSTRACT

A one-step, hydrothermal method for the synthesis of nitrogen, carbon co-doped titanium dioxide (N,C—TiO_2) photocatalysts is demonstrated. The incorporation of nitrogen from ammonia and carbon from alcohols with different chain length (methanol, ethanol, isopropanol, 1-butanol, 2-butanol, tert-butanol) used as carbon precursors was confirmed by FTIR/DRS and XPS analyses. The UV–vis/DR absorption spectra of the modified photocatalysts extended into the visible. XRD, BET and Zeta Sizer-Nano techniques were used for the characterization of the modified photocatalysts. The crystallite size of N,C—TiO_2 was not affected by the nature of the alcohol or the pressure acquired during the modification process but surface area, particle size (crystal agglomerate) and anatase content increased with synthesis pressure. In contrast with other studies in literature, the photoactivity of the different synthesized materials was evaluated at a constant volumetric rate of photon absorption (VRPA) in an annular photoreactor. This innovative method allows the evaluation of the intrinsic photoactivity of each material. As a result, the effect of N,C-co-modification on the TiO_2 photoactivity was evaluated without interference from the amount of radiation absorbed by each suspended powder since the total radiant energy absorbed by each slurry suspension was kept constant. Phenol decomposition confirmed that activity increased with the chain length of the alcohol precursor. The highest intrinsic photoactivity was for N,C—TiO_2 prepared from 2-butanol, and 1-butanol as carbon precursor which also exhibited much stronger resistance to deactivation during multiple catalyst reuse compared to pristine TiO_2 and commercial Degussa P25 photocatalysts.

1. Introduction

Titanium dioxide (TiO_2) is a widely used photocatalyst for water treatment, air purification, antibacterial, deodorization, self-cleaning coating or anti-stain applications [1–5]. The irradiation of TiO_2 with band gap photons produce electron–hole couples which after migration to the surface of the solid may be trapped by surface reducible species (e.g., molecular oxygen) and adsorbed water to produce superoxide anion radicals and hydroxyl radicals. Subsequent reactions of these radicals between themselves and with adsorbed molecules lead to oxidation/reduction reactions which in turn may degrade aqueous/air pollutants. The band-gap of TiO_2 (anatase) is 3.2 eV, in consequence photons of wavelength of 384 nm or less (UV-A) can promote the generation of electron–hole couples. However, the redox process is limited by electron–hole recombination which in practice reduces the effectiveness of TiO_2 as a photocatalyst. The narrowing of the band gap in TiO_2 and its modification allows the utilization of a wider fraction of visible light for the production of charge carriers. Metal ions (Pt, Au, Ag, Cu, Fe), metal oxides (SnO_2, WO_3, MnO_2, V_2O_5) and nonmetals (C, N, F, S, P) have been proposed as modifiers that improve the photoactivity of TiO_2 [5–14]. Nitrogen and carbon doped into substitutional sites of TiO_2 [15] results in narrow band gaps (red-shift) which may lead to higher photo-response and higher photocatalytic activity. In other studies it is revealed that doped TiO_2 undergoes electronic transitions from localized states near the valence band to their corresponding excited states for Ti^{3+} centers after visible light irradiation [[16] and reference therein]. Co-doping of titania with carbon and nitrogen simultaneously [17–28] may also show synergistic effect.

In the study by Yin et al. [17] N and C co-doped titania prepared by a mechano-chemical method revealed very high photocatalytic activity for nitrogen monoxide degradation under visible light irradiation, possessing two absorption edges around 400 nm and 540 nm. Chen et al. [18] synthesized TiO_2 photocatalysts with different amounts of carbon and nitrogen by the sol–gel method. The

* Corresponding author. Tel.: +44 0 1509222510; fax: +44 0 1509223923.
E-mail address: g.lipuma@lboro.ac.uk (G. Li Puma).

0926-3373/$ – see front matter © 2011 Elsevier B.V. All rights reserved.
doi:10.1016/j.apcatb.2011.12.007

Table 1
Physico-chemical properties and band gaps of pristine TiO_2 and of N,C—TiO_2 catalysts.

	Photocatalyst						
	Pristine	N,C—TiO_2/NH_4OH, alcohol					
		Methanol	Ethanol	Isopropanol	1-Butanol	2-Butanol	Tert-butanol
Modification pressure (bar)		3.8	4	6.8	7.2	9.4	7.4
% Anatase in crystalline phase	87.5	90.2	90.4	91.8	91.7	93.5	91.6
% Rutile in crystalline phase	12.5	9.8	9.6	8.2	8.3	6.5	8.4
Anatase crystallite size (nm)	12	16	17	19	18	19	19
Particle size (nm)	184	207	210	220	183	171	211
BET surface ($m^2\ g^{-1}$)	238	108	114	145	166	179	113
Band-gap energy (eV)	3.49	3.43	3.44	3.21	3.10	3.11	3.51

increase of photocatalytic degradation of methylene blue under visible light irradiation was ascribed to the synergistic effect of C and N atoms in agreement with other researchers [19–23]. Zhang et al. [23] proposed that the degradation of methylene blue under visible light was the results of partial replacement of oxygen atoms on the TiO_2 surface with nitrogen, whereas the carbon atoms formed a mixed layer of deposited carbon and C—O band species on the surface of the TiO_2 particles. N and C co-doping of titania may also lead to an increase of the BET surface area of the catalyst [20] and improved photoactivity in the visible and UV regions. Carbon and nitrogen may act as photosensitizers. The substitution of oxygen atoms by nitrogen in the TiO_2 structure improves the absorption of visible light by mixing the N2p and O2p states and/or introducing a mid-gap N2p level which is located above the top of the O2p valence band. Serpone [16] proposed that the red-shift of the absorption edge is due to the formation of color centers, including Ti^{3+} centers and defects associated with oxygen vacancies that give rise to color centers displaying these absorption bands. He argues against the narrowing of the original band-gap of TiO_2 resulting from the mixing of dopant and oxygen states as that would require heaving of an anion or cation doping. Tseng et al. [25] showed the role of the chamber atmosphere on the surface lattice structure and nitrogen and carbon content of titania prepared by a metal-organic chemical vapor deposition process and the effect on NO photooxidation by visible-light. Wang et al. [26] described the degradation of bisphenol A by visible LED light in the presence of N,C co-doped TiO_2 prepared by solvothermal synthesis.

In this study specimens nitrogen–carbon co-doped anatase titania with different optical and structural characteristics were prepared by a simple, one-step hydrothermal method with different alcohols as carbon precursors and in the presence of ammonia water (NH_4OH) vapors as the nitrogen precursor. The effect of the alcohol degree and chain length employed for C-doping was investigated. In contrast with other studies in literature, the photoactivity of the different synthesized materials was evaluated at a constant volumetric rate of photon absorption (VRPA) in the photoreactor. This different method allows the evaluation of the intrinsic photoactivity of each material. As a result, the effect of N,C-co-modification on the TiO_2 photoactivity was evaluated more accurately without interference from the amount of radiation absorbed by each suspended powder.

2. Experimental

2.1. Materials

Commercial P25 TiO_2 (Degussa, Germany) with BET surface area of 55.5 $m^2\ g^{-1}$ was used as a reference photocatalyst. A commercial titanium dioxide (TiO_2/A) supplied by Chemical Factory "Police" S.A. (Poland) with BET surface area of 238 $m^2\ g^{-1}$ was used as a pristine material for the synthesis of N,C modified TiO_2. Alcohols (methanol, ethanol, isopropanol, 1-butanol, 2-butanol, tert-butanol, POCH, Gliwice, Poland) and ammonia water (30%, reagent grade, ACS, ISO, Scharlau Chemie) used as carbon and nitrogen precursors of N,C—TiO_2, were of analytical grade or of higher purity. Phenol (Sigma–Aldrich, 99.5%) was the model organic pollutant for the evaluation of the photocatalysts activity. High purity water for the photocatalytic experiments and sample analysis was produced by a Millipore Milli Q water purification system that provides bacteria free water at 18 M cm^{-1} resistivity and with less than 1 ppb total organic carbon.

2.2. N,C co-doping procedure

Modification of TiO_2 was conducted in a one-step process with different alcohols as carbon precursors and in the presence of ammonia water (NH_4OH) vapors as the nitrogen precursor. The description of the pressure reactor employed in this work is shown elsewhere [29,30]. 4 g of TiO_2/A and 5 mL of the selected alcohol were placed inside the reactor vessel, 5 mL of ammonia solution was added and the reactor was closed and heated up to 100 °C. The system was kept at this temperature for 4 h. The maximum pressure and the anatase–rutile composition obtained during each modification are shown in Table 1. It varied between 3.8 and 9.4 bar depending on the type of alcohol used. After the thermal treatment was completed the reactor was cooled down slowly for 20 h to room temperature. Subsequently, the N,C-modified TiO_2 photocatalysts were dried for 24 h at 105 °C in a muffle furnace and stored in sealed bottles for further use.

2.3. Photocatalyst characterization

The photocatalysts were characterized by UV–vis/DR technique using a Jasco V-650 spectrophotometer (Japan) equipped with an integrating sphere accessory for diffuse reflectance spectra acquisition ($BaSO_4$ was used as a reference). The surface properties of the photocatalysts were examined by means of FTIR/DRS spectrometry. Measurements were performed using a Jasco FTIR 4200 (Japan) spectrometer equipped with a diffuse reflectance accessory (Harrick, USA). The crystalline structure of the photocatalysts was characterized by X-ray powder diffraction (XRD) analysis (X'Pert PRO Philips diffractometer) using Cu Kα radiation. The N_2-BET specific surface area of the photocatalysts was measured at 77 K using a Quadrasorb SI (Quantachrome Instruments, U.S.A.) instrument. Prior to analyses, each sample was degassed at 105 °C for 24 h under high vacuum. The values of the specific surface areas (S_{BET}) were determined using multi-point analysis of adsorption isotherms applying Brunauer–Emmet–Teller (BET) equation. The average particle size was evaluated using a ZetaSizer Nano Nano-ZS (Malvern Instruments) which uses dynamic light scattering (DLS). The particle size distribution of the catalyst was evaluated from the Brownian motion of the particles. XPS analyses were carried out in

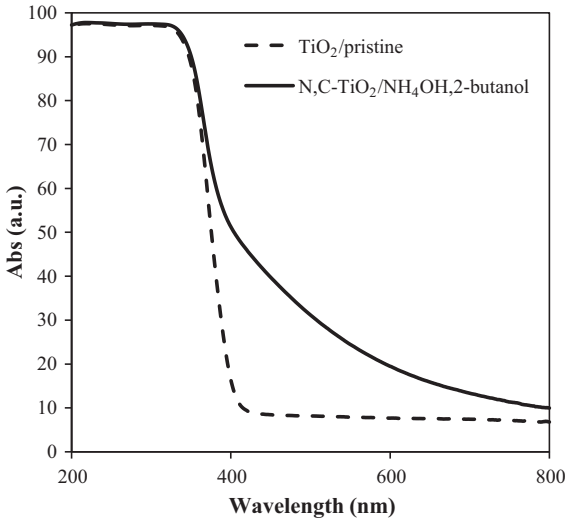

Fig. 1. UV–vis absorption spectra of pristine TiO_2 (dashed line) and N,C-TiO_2 modified with NH_4OH,2-butanol (solid line).

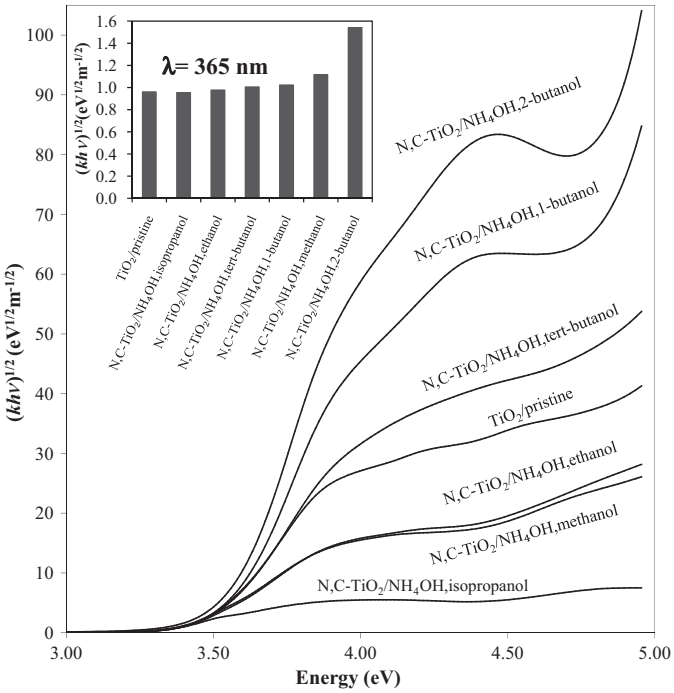

Fig. 2. UV–vis/DRS spectrum plotted using the Kubelka–Munk model. The inset shows the K–M values obtained for each catalyst at λ = 365 nm.

a PREVAC electron spectrometer equipped with SES 2000 (VC Scienta) electron energy analyzer. Samples were excited by Mg Kα X-ray radiation.

2.4. Photoreactor and experimental procedures

The photocatalytic activity of the catalysts was evaluated by monitoring the degradation of phenol. Irradiation experiments were performed in a batch recirculation system consisting of an annular photoreactor, a pulse-free peristaltic pump and a well-mixed recirculation vessel. The outer wall of the annular photoreactor was a QVF borosilicate glass tube (internal diameter 0.038 m, wall thickness 0.0045 m) while the inner wall consisted of a replaceable Pyrex tube (external diameter 0.026 m) mounted at the axial center of the reactor. The radiation wavelength cut-off of the Pyrex tube was found to be 300 nm. The length of the reaction zone in the annular photoreactor was 0.255 m. The irradiated volume of suspension ($V_{reactor}$) was 0.134 L. A Philips blacklight-blue TL 8W/08 F8 T5/BLB lamp (nominal power 8 W, bulb length 0.213 m, bulb radius 0.007525 m) was mounted axially inside the Pyrex tube and centered with respect to the length of the reactor. The ends of the lamp were covered with Teflon tape to expose a central section, 0.213 m in length, emitting constant radiation per unit length. This lamp emits radiation between 323 and 406 nm with a peak at 365 nm (Fig. S1 in Supplementary data). The photon flux from the lamp was controlled using a variable power supply unit and measured using a microprocessor-controlled radiometer (Cole-Parmer) fitted with a 365 nm UVA sensor (range 355–375 nm; sensors accuracy ± 5%; display accuracy ± 0.2% at full scale). The photon irradiance at the wall of the lamp averaged across the emission spectrum was estimated following the method in [31] and was 86.96 W m^{-2} for pristine TiO_2 (wavelength range 323 nm < λ < 384 nm) and 95.07 W m^{-2} for the N,C co-doped TiO_2, since the absorption spectrum extends into the visible (wavelength range 323 nm < λ < 406 nm). The reactor was operated in a recirculating batch mode, whereby reactants continuously passed through the reactor and were fed back to a well-mixed recirculation vessel. The rig was covered by a protective black curtain to avoid exposure of personnel to UV radiation. The schematic diagram of the photocatalytic reactor setup has been presented elsewhere [31].

In each experiment, the N,C-modified TiO_2 powder was initially suspended in 2 L of a 5 ppm phenol aqueous solution. Once transferred to the recirculation tank, the suspension was stirred for 1 h in the dark to reach equilibrium of the adsorption of phenol onto the catalyst. The experiments were carried out at ambient temperature (22 °C). Samples were withdrawn at regular intervals, filtered through 0.45 μm nylon filters and analyzed. The filter material did not retain phenol. Phenol concentration in the solution was determined using a UV–vis mini 1240 spectrophotometer at 269 nm.

When the degradation of phenol was complete, the UV lamp was turned off and phenol was added to the suspension to raise again its concentration to 5 ppm and another cycle of photocatalytic degradation was performed. It should be noted that reaction intermediates either adsorbed on the photocatalyst surface or in solution accumulated after each cycle in the reactor. This procedure was followed to evaluate the activity and the rate of catalyst deactivation. When three consecutive cycles were completed the suspension was filtered and the separated photocatalyst was dried at room temperature. The photocatalyst surface after the process was analyzed by FTIR to examine surface changes and the presence of carbon deposits.

3. Results and discussion

3.1. UV–vis/DR

Fig. 1, shows the UV–vis/DR spectra of pristine TiO_2 together with the spectra obtained for N,C—TiO_2/2-butanol. Pristine TiO_2 absorbed radiation in the ultraviolet, however, the absorption spectra of the modified photocatalysts extended into the visible. The UV–vis/DR spectra for all the samples was plotted using the Kubelka–Munk model [32] that allows the calculation of the reflectance from materials that both scatter and absorb light. This so-called "two-flux" model, where only diffuse light is considered [33], is appropriate when strong photon scattering takes place, with diffuse incident light or when surfaces are optically rough [34]. The raw UV–vis reflectance data could not be used directly to assess the absorption coefficient of the TiO_2 powders

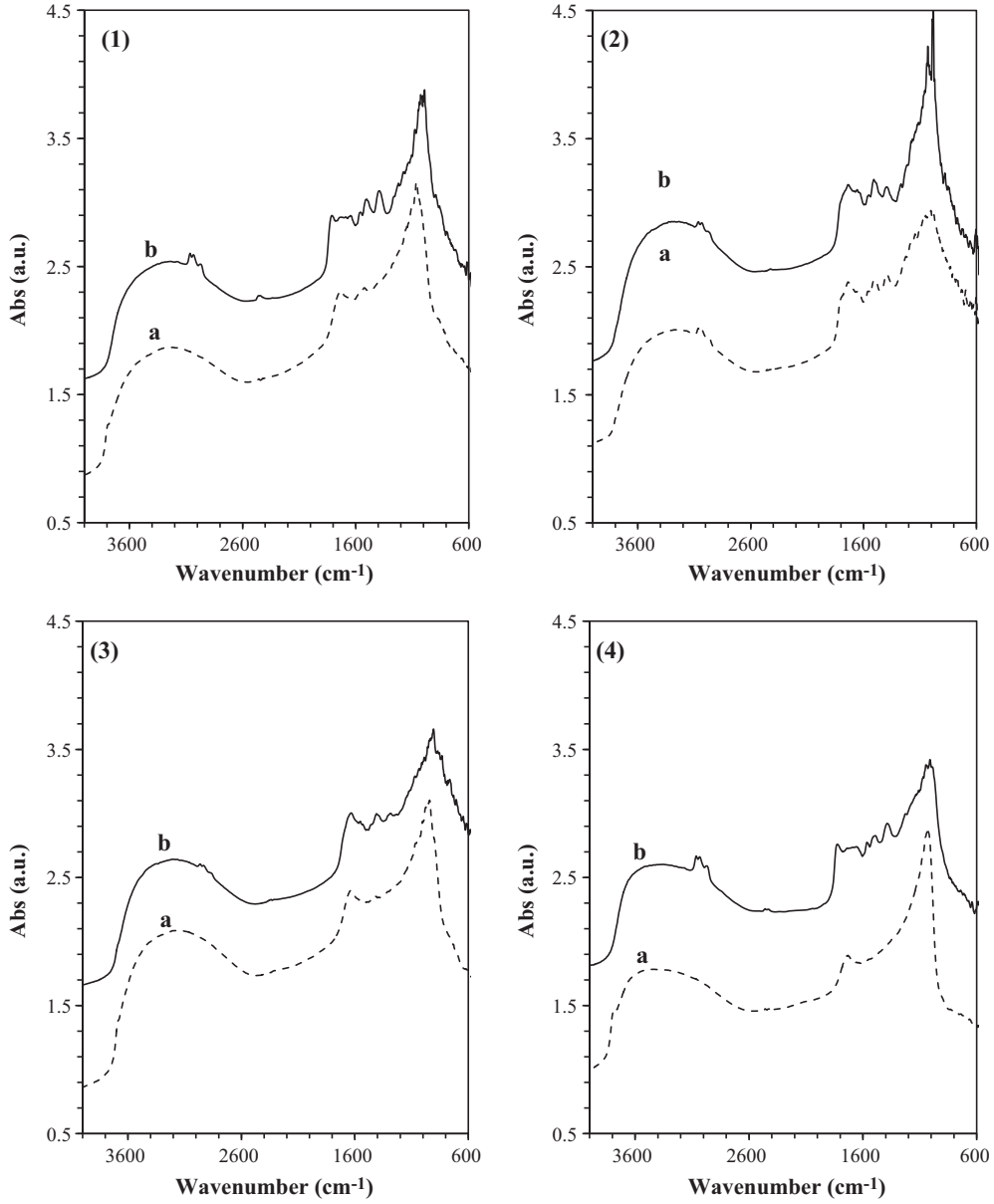

Fig. 3. FTIR/DRS spectra of selected photocatalysts before (a) and after (b) photocatalytic process; (1) N,C—TiO_2/NH_4OH,methanol; (2) N,C—TiO_2/NH_4OH,2-butanol; (3) TiO_2/pristine; (4) commercial Degussa P25.

because of the large scattering contribution to the reflectance spectra [35] but it was possible to derive the absorption coefficient from measurements of the diffuse reflectance of the sample by inverting the Kubelka–Munk expression for the diffuse reflectance. The dependence of the absorption coefficient K on the frequency, ν, of crystalline solids with an indirect band gap (i.e., anatase TiO_2) can be approximated as:

$$Kh\nu = A(h\nu - E_g)^2 \quad (1)$$

where A is a constant, E_g is the band gap energy and h is the Planck constant [33].

Fig. 2 shows the plot of $(Kh\nu)^{1/2}$ against energy obtained from the UV–vis/DR spectra of the N,C—TiO_2 catalysts prepared from different carbon precursors. The light absorption edges of the catalysts prepared from NH_4OH/2-butanol and NH_4OH/1-butanol were shifted towards longer wavelengths more significantly than in the other catalysts. Table 1 shows the band gap energy of the catalysts estimated from Fig. 2. In addition, the absorption in the UV region was stronger (the inset in Fig. 2 shows the $(Kh\nu)^{1/2}$ values obtained at 365 nm). Therefore, the carbon/nitrogen co-modification of these two photocatalysts was highly effective in promoting their photo-response. Stronger photon absorption was observed in the specimens prepared with longer alcohol chain lengths, which results from the higher amount of carbon doping in the TiO_2.

3.2. FTIR/DRS

The surface properties of the photocatalyst were investigated by FTIR/DRS. Fig. 3 shows the FTIR/DRS spectra of N,C—TiO_2 prepared from NH_4OH/methanol (1) and NH_4OH/2-butanol (2) together with the spectra of TiO_2/pristine (3) and TiO_2 Degussa P25 (4). The spectra of the N,C—TiO_2 prepared from NH_4OH/ethanol and NH_4OH/ter-butanol were almost identical to those prepared from NH_4OH/methanol (not shown). Similarly, the spectra of N,C—TiO_2 prepared from NH_4OH/1-butanol was similar to the one prepared

from NH_4OH/2-butanol. The spectra of N,C—TiO_2 prepared from NH_4OH/isopropanol did not show additional bands compared to the spectra of the photocatalysts prepared from 2-butanol and methanol. Some bands are common to all the materials presented: the broad band at 2500–3700 cm^{-1} [36] and narrow band at 1640 cm^{-1} were assigned to the hydroxyl group [37]. The narrow band at 1440 cm^{-1} in the synthesized catalysts was attributed to the ammonium groups (NH_4^+) [37], which suggests that nitrogen was successfully incorporated into the structural lattice. Nevertheless, the bands at 1440 cm^{-1} could also be attributed to the CO group [38] or could be a resultant of both NH_4^+ and CO bands. A new band at 1540 cm^{-1} appeared in the spectra of N,C—TiO_2 photocatalysts prepared from 1-butanol, 2-butanol and isopropanol. This band can be ascribed to either NH_2 or NO_2 and NO groups [39]. Besides the nitrogen modification, the presence of carbon containing groups on the catalysts surface was confirmed in these new materials. New carbon bands on the TiO_2 surface at 1400 cm^{-1} (CH_2 scissors), and at 1295 cm^{-1} (CH groups) could be seen in the spectra of the materials prepared from 1-butanol, 2-butanol and isopropanol. In addition, new carbon containing methyl groups were observed in the 3010–2860 cm^{-1} regions for N,C—TiO_2 prepared from 1-butanol and 2-butanol.

Fig. 3 also shows the catalyst spectra before (a) and after (b) three cycles of phenol photocatalytic decomposition. The carbon deposits increased after the photocatalysis of phenol when N,C—TiO_2/NH_4OH, methanol and TiO_2 P25 were used. We attribute this effect to the relatively low activity of these catalysts observed and to the presence of a larger fraction of rutile phase in the catalyst structure, which is more evident in the P25 specimen. The rutile phase of TiO_2 does not exhibit particularly high photocatalytic properties for the removal of water contaminants [40,41] which in turn results in larger amounts of carbon deposits on its surface that cannot be completely oxidized during the photocatalytic degradation process. The distinctive bands on the new catalysts were stable during the photocatalytic degradation processes. New bands originating from the nitrogen and/or carbon pressure modification process were observed in the FTIR/DRS spectra of the modified catalysts before and after three cycles of phenol decomposition. This fact leads to the conclusion that the incorporation of non-metals (N and C) into the catalyst structure was strong enough to be stable during the photocatalytic process. These new groups that build up on the photocatalysts surface can thus provide long-lasting photocatalytic activity preventing catalyst deactivation. These results confirm the conclusions made after the UV–vis/DRS analysis.

The samples were also analyzed by XPS and the results supported the hypothesis of the incorporation of nitrogen in the new materials. Fig. 4 shows the XPS spectra of N,C—TiO_2 when 2-butanol was used as C modifier. A peak corresponding to nitrogen can be observed in the inset figure showing binding energies between 395 and 410 eV (the spectra obtained for pristine TiO_2 is shown for comparison). In general, the peak of N1s in the XPS spectra mostly lies in the range of 396–404 eV but this can shift depending on the preparation method of the N,C-modified catalysts [42].

3.3. XRD, BET surface area and particle size

The degree of crystallinity, the anatase/rutile phase ratio, the size of the crystallite and particle agglomerates, and the catalyst surface area can significantly influence the efficiency of photocatalytic oxidation of water contaminants. Fig. 5 shows the X-ray diffraction patterns of the photocatalysts. Table 1 presents the percentage of anatase and rutile phase, crystallite size, particle size and BET surface area of the photocatalysts obtained with different carbon precursors. It can be observed that the pressure modification at 100 °C caused an increase of the anatase phase and a decrease of the amorphous phase. The percentage of anatase

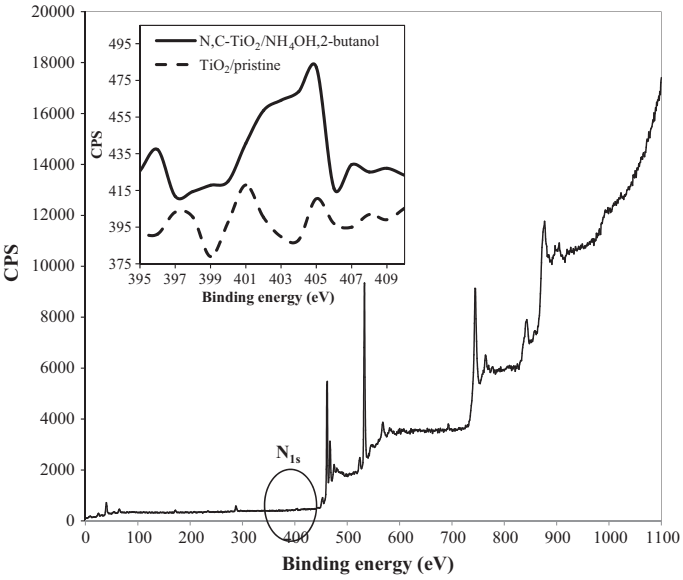

Fig. 4. High-resolution XPS of N,C—TiO_2/NH_4OH,2-butanol. The insert shows a comparison between the XPS spectra of pristine TiO_2 (dashed line) and doped TiO_2 (solid line) in the region of N1s peak.

correlated with the synthesis pressure and as it will be discussed later, these materials also exhibited the highest photocatalytic activity with the exception of tert-butanol modified catalyst. The mean crystallite size was calculated from full width at half maxima (FWHM) of the corresponding X-ray diffraction anatase peak located at 27.5° using Scherrer's formula,

$$D = \lambda(\beta \cos\theta)^{-1} \quad (2)$$

where λ is the wavelength of the X-ray radiation (λ = 1.54056, Cu Kα), β is the full width at half maximum (rad) and θ is the reflected angle. The width of the peak at half maximum was calculated after correction of the instrument error [43]. Therefore, larger surface areas (i.e., smaller particle sizes) were obtained in the photocatalysts with higher anatase content and, as confirmed by UV–vis/DR and FTIR/DRS spectra, these materials also were those with the highest carbon content. Furthermore, it is shown that the crystallite size of the N,C—TiO_2 materials remained constant regardless of the nature of the alcohol precursor or the pressure acquired during the modification process. While the crystallite size of the modified catalysts was almost constant, the particle sizes and surface areas change simultaneously (Fig. 6). It can be concluded that the change in particle size was caused by the modification of the material

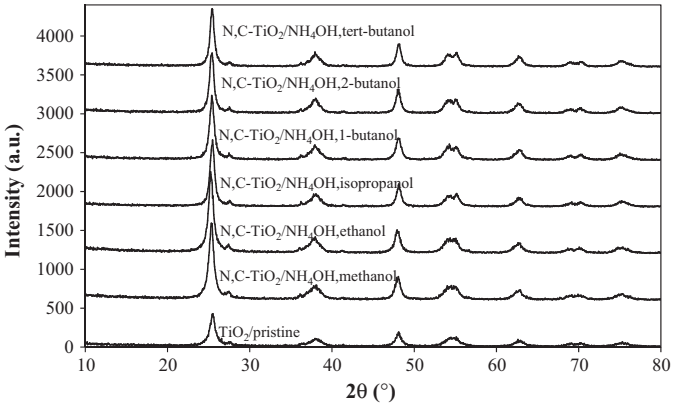

Fig. 5. Powder X-ray diffraction patterns of the N,C-co-doped photocatalysts measured with Cu Kα.

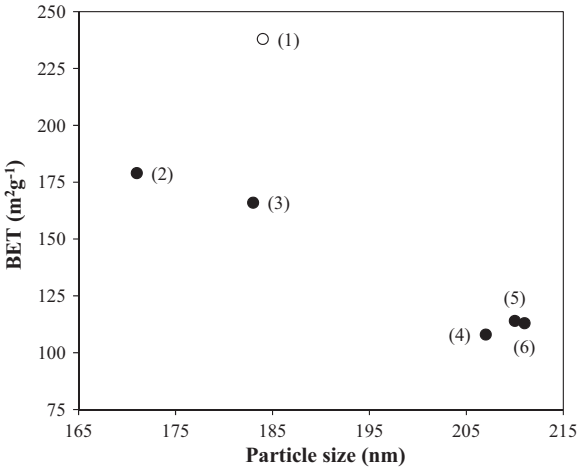

Fig. 6. BET surface area and particle size for TiO_2/pristine (1) and for the different N,C—TiO_2 materials modified with: (2) NH_4OH/2-butanol; (3) NH_4OH/1-butanol; (4) NH_4OH/methanol; (5) NH_4OH,/ethanol; (6) NH_4OH/tert-butanol.

surface. As the carbon content on the surface increased, the surface charge decreased reducing particle agglomeration and, as a result, smaller particle size and larger surface areas were obtained.

3.4. Photocatalytic activity and kinetics

In an irradiated suspension of photocatalytic particles photons are absorbed and scattered. Thus, the photocatalytic activity depends on the efficiency of utilization of the fraction of the incident radiation absorbed by the catalyst, which results in the generation of electron/hole couples. The intrinsic kinetic parameters of photocatalytic reactions, independent from the rate of photon absorption and radiation flux, can be determined only with the knowledge of the radiation field in the photoreactor, which, between other factors, strongly depends on the optical properties of the photocatalysts [31,44,45]. In the majority of kinetics studies, photocatalytic activity of different photoactive materials have been compared at equal catalyst concentration (i.e., mass of the catalyst added to the photoreactor). However, the rate of a photocatalytic reaction is a strong function of the total radiant energy absorbed by the catalyst in suspension, which in turn depends on the geometry of the photoreactor (configuration and lamp arrangement) and on the optical properties (absorption and scattering coefficients) of the photocatalyst. Since photons are essential to the process of photocatalysis (i.e., without photons there is no photocatalysis!) a comparison of the photocatalytic activities of different modified oxides cannot be carried out solely by performing experiments at constant catalyst concentration, since different materials unveil different optical properties. It is well documented that the optical properties of photoactive materials depend on the crystallite size, the crystal phase and strongly on the size of the particle agglomerates in an aqueous suspension [40,46–49]. As shown in Table 1, the different materials had the same crystallite size but different particle agglomerates. As a result, these materials displayed different optical properties. In consequence, a comparison of the photocatalytic activities based on the same mass of catalyst loaded into the photoreactor would have produced inconclusive results regarding their intrinsic photoactivity. To address the above limitations, avoiding the precise measurements of the optical properties of the catalysts which require specialized equipment [40], the photocatalytic activity of each material was evaluated keeping constant the total radiant energy absorbed by each slurry suspension. In other words, the rate of photon absorption averaged across the entire irradiated reactor volume was kept constant during the experiments with each photocatalytic material. In practice, this can be easily realized by adding the correct amount of catalyst in the suspension until the photon irradiance emerging from a particular reactor wall transparent to UV radiation remains equal. Since the lamp was enclosed in the center of the annulus, it was assumed that most of the back-scattered photons were recaptured by the catalyst suspension in the annulus where they can undergo further absorption and scattering. Those back scattered photons re-entering the lamp bulb are absorbed and re-emitted. The only photon losses from the reactor enclosure occurred through either the external wall of the annulus or the narrow top and bottom sections of the annular reactor. The blacklight lamp emitted UV-A radiation and visible light up to 406 nm which could be totally absorbed by the N,C-modified TiO_2 powders. In contrast, the unmodified anatase TiO_2 absorbed radiation up to 384 nm, therefore, the photon irradiance measured by the UV-A sensor at the lamp wall was slightly higher in the experiments performed with the N,C-modified TiO_2 powders to account for the extra photons that were emitted in the 385–406 nm interval (9% of the total radiation emitted by the lamp). Table 2 shows the catalyst concentration which was needed to reach the same proportion of photon absorption in the annular reactor with each of the catalysts. It varied significantly from 0.05 g L^{-1} for N,C—TiO_2 photocatalyst prepared from 2-butanol to 0.39 g L^{-1} for pristine TiO_2. Since the total radiant energy emitted by the lamp in the UV-A region of the spectrum remained constant, the same volumetric rate of photon absorption was realized with each catalyst suspension and therefore an intrinsic comparison of the photocatalytic activities of these materials could be made.

The results in Table 2 show that the materials with the strongest photon absorption followed the order: N,C—TiO_2, 2-butanol > N,C—TiO_2, 1-butanol > N,C—TiO_2, ethanol, TiO_2 P-25 > N,C—TiO_2, isopropanol, N,C—TiO_2, methanol > N,C—TiO_2, 3-butanol > pristine TiO_2. Note that a similar trend is observed in the inset of Fig. 2, showing the Kubelka–Munk values obtained for the different catalyst at $\lambda = 365$ nm. The radiation absorption properties of the catalysts are also influenced by the nitrogen and carbon modification efficiency and by the catalyst particle size (i.e., surface area). The results show that the materials modified with longer chain alcohols absorbed more photons. The UV–vis/DR and FTIR/DRS results showed that the carbon modification efficiency and surface area (particle size) follow almost the same order. It can be concluded that these properties of the materials complement each other to yield higher photoactivity. The N,C—TiO_2 prepared from 2-butanol and 1-butanol presented the smaller particle size (i.e., larger surface area) and the highest photon absorption properties. The N,C co-doping of TiO_2 shifted the light absorption of TiO_2 from the UV into the visible but this also resulted in a variation of the absorption coefficient (K) in the UV region. Therefore, the photocatalytic experiments were performed with UV-A irradiation since the aim was to evaluate the performance and lifetime of the catalysts under conditions that could be compared with the two reference materials, pristine TiO_2 and commercial Degussa P25.

The decomposition of phenol was followed to probe the photocatalytic activity of the catalysts (Fig. 7). In the first degradation cycle, the degradation kinetics were pseudo first-order (Eq. (3)) up to ca. 75% conversion with rather good correlation coefficients ($R^2 > 0.9$).

$$-r = k_{app}C \tag{3}$$

The rate constants per unit reactor volume (k_{app}) were obtained by fitting the experimental data. An apparent first-order kinetics is realized when the Langmuir–Hinshelwood rate equation is simplified at low phenol concentration to make the term $KC \ll 1$ where K is the isothermal adsorption constant of phenol onto the catalyst and C is the concentration of phenol. Note that k_{app} includes the effect of radiation absorption, however, since all experiments were

Table 2
Photocatalyst concentration (C_w) that achieves the same volumetric rate of photon absorption in the annular reactor and apparent rate constants of phenol degradation per unit reactor volume (k), per gram of catalyst (k_w) and per unit surface area of catalyst (k_s) after up to three consecutive photocatalytic cycles of phenol degradation.

		P25	Pristine	N,C—TiO_2/NH_4OH, alcohol					
				Methanol	Ethanol	Isopropanol	1-Butanol	2-Butanol	Tert-butanol
	C_w (g L^{-1})	0.10	0.39	0.17	0.10	0.16	0.09	0.05	0.23
1st cycle	$k \times 10^2$ (min^{-1})	8.06	5.07	3.58	4.33	6.12	5.37	3.88	4.03
	$k_w \times 10^2$ (min^{-1} g^{-1})	40.30	6.51	10.54	21.64	19.12	29.85	38.81	8.76
	$k_s \times 10^2$ (min^{-1} m^{-2})	0.72	0.03	0.10	0.19	0.13	0.18	0.22	0.08
2nd cycle	$k \times 10^2$ (min^{-1})	4.78	2.24	2.39	4.33	6.12	5.37	3.88	3.88
	$k_w \times 10^2$ (min^{-1} g^{-1})	23.88	2.87	7.02	21.64	19.12	29.85	38.81	8.44
	$k_s \times 10^2$ (min^{-1} m^{-2})	0.43	0.01	0.07	0.19	0.13	0.18	0.22	0.07
3rd cycle	$k \times 10^2$ (min^{-1})	4.63	2.24	2.39	4.33	5.52	5.37	3.88	3.28
	$k_w \times 10^2$ (min^{-1} g^{-1})	23.13	2.87	7.02	21.64	17.26	29.85	38.81	7.14
	$k_s \times 10^2$ (min^{-1} m^{-2})	0.41	0.01	0.07	0.19	0.12	0.18	0.22	0.06

carried at equal level of photon absorption this effect is the same for all catalysts investigated. Note that this aspect is not taken into account in many studies in literature that compare the activities of different photocatalysts. The annular photoreactor was considered to be a differential reactor since the degradation rates per pass were small. In consequence, the material balance on phenol in the batch recirculation system consisting of the annular photoreactor and the well mixed recirculation vessel reduces to:

$$\frac{V_{total}}{V_{reactor}}\frac{dC}{dt} = r \quad (4)$$

where V_{total} is the total volume of liquid in the system (2 L) and $V_{reactor}$ is the irradiated volume of the reactor (0.134 L).

After integration the first-order rate constant k_{app} per unit reactor volume was estimated from the linear fitting of the plot of $-\ln(C/C_0)$ versus the reaction time t, where C_0 is the initial concentration of phenol.

$$k_{app} = \frac{V_{total}}{V_{reactor}} \times \text{slope} \quad (5)$$

The apparent rate constants of the catalyst per unit mass k_w and per unit surface area k_s were estimated from Eqs. (6)–(7):

$$k_w = \frac{k}{C_w V_{total}} \quad (6)$$

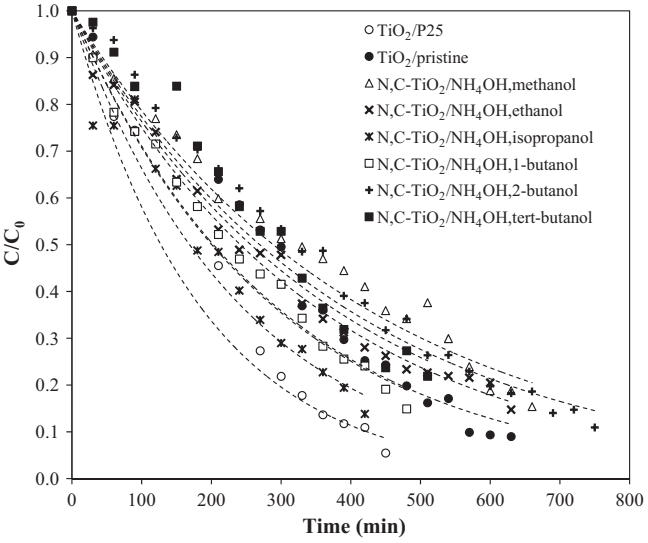

Fig. 7. Photocatalytic activity of the TiO_2/P25, TiO_2/pristine and N,C—TiO_2 photocatalysts for the degradation of phenol (C_0 0.053 mM), first cycle.

$$k_s = \frac{k}{A_c C_w V_{total}} \quad (7)$$

where C_w is the concentration of photocatalyst and A_c is the BET surface area.

Table 2 shows the observed rate constants of the catalysts, per unit reactor volume ($k = k_{app}$), per gram of catalyst (k_w) and per unit surface area (k_s). It can be seen that the rate constants per gram of catalysts (1st cycle) are the highest for N,C—TiO_2/NH_4OH, 2-butanol, N,C—TiO_2/NH_4OH, 1-butanol. This higher performance may be attributed to the highest anatase content, the smallest particle sizes (see Table 1) and also their carbon modification that was proved to be the most effective in changing the structural properties of these catalysts. TiO_2 P25, used here for comparison purposes, was the most effective of all catalysts during the 1st cycle of phenol degradation.

3.5. Photocatalysts reuse/deactivation

Each catalyst was reused twice, leading to three cycles of reactions to assess the resistance of the catalysts to deactivation. The k_{app} calculated from the kinetics plots obtained after the second and third cycles (which deviated further from an apparent first-order due to the accumulation of intermediates after each cycle) were compared to the k_{app} of the first cycle to evaluate the potential of the material for continuous reuse.

The activity of TiO_2 Degussa P25 for phenol degradation decreased significantly after each photocatalytic cycle in comparison with the N,C-co-doped catalyst, particularly, when 1-butanol and 2-butanol were used as C precursors (Table 2). This effect may be caused by a higher amount of carbon deposits on the P25 surface generated by significant amounts of inactive rutile phase in the photocatalysts structure as observed by Janus et al. [50]. Conversely, N,C—TiO_2/NH_4OH, 2-butanol and N,C—TiO_2/NH_4OH, 1-butanol catalysts exhibited superior resistance to deactivation. The decrease of activity found for the catalyst modified with methanol, tert-butanol and isopropanol could be assigned to a loss in surface active sites as a result of the poisoning of the catalyst from the by-products formed during the degradation of phenol which were adsorbed onto catalyst surface. However, changes in activity of the N,C-co-doped catalysts were statistically insignificant. Furthermore, the rate constants per unit mass of N,C—TiO_2/NH_4OH, 2-butanol and N,C—TiO_2/NH_4OH, 1-butanol were much higher than the one for TiO_2 P25 suggesting a more viable use of these materials compared to the commercial catalyst.

3.6. Further considerations on the evaluation of catalyst activity at equal rate of photon absorption

The method of measuring the irradiance at the outer wall of an annular photoreactor has been reported in literature to estimate an optimal catalyst concentration for the evaluation of the activity of one or more TiO_2 catalysts [51,52]. The method was used to confirm that the catalyst suspension in the reactor was fully irradiated by photons and that a maximum rate of photon absorption was approached. However, the interpretation of the results may be affected by the difficulty of relating photon absorption to photoactivity since the comparison of different catalysts is usually performed at a fixed number of catalyst concentrations. The new method that we present here circumvents these difficulties since it evaluates catalyst activity at an approximately equal rate of photon absorption with each catalyst suspension. However, it should be observed that this method should only be adopted when the photocatalyst is operating under unsaturated conditions (i.e., at low pollutant concentrations to approximate common Langmuir–Hinshelwood (L–H) type kinetics to an apparent first-order kinetics) to avoid reaction kinetics being affected by the degree of saturation of the catalysts. If such condition of complete saturation of the catalyst becomes inevitable (e.g., high pollutant concentration and L–H kinetics approximating apparent zero-order kinetics) the catalyst concentration should then be increased to re-establish the conditions of unsaturation of the catalytic sites, and simultaneously, the thickness of the reactor traversed by photons (i.e., for an annular reactor the thickness of the annulus) should be reduced to compensate for the increased opacity, and therefore, to continue to operate the reactor under optimal radiation absorption conditions. It is well known that the optimal absorption of photons should be realized at an optimal value of the optical thickness, τ [53]. Therefore, since optical thickness depends on catalyst concentration and reactor thickness, then, if the catalyst concentration is increased the reactor thickness must be reduced by an equal proportion. These simple engineering considerations should be useful to evaluate catalyst photoactivity in laboratory and full scale reactors.

4. Conclusions

In summary, this study has demonstrated a simple one-step method for the synthesis of N,C-modified TiO_2 photocatalysts. The incorporation of N from ammonia and C from alcohols into the photocatalysts was confirmed by FTIR/DRS and XPS studies. The nature of the alcohol used as C precursor was found to have a significant role on the optical (absorption of radiation) and physico-chemical (surface area, particle and crystallite size) properties of the modified materials.

A new approach for the evaluation of the intrinsic photocatalytic activity of the catalysts, based on equal VRPA of the slurry suspensions was proposed. This approach should be adopted for the evaluation and ranking of photocatalysts without interference from the radiation absorbed by each material in the photoreactor. It is equivalent to the estimation of quantum yield but in this approach the same level of VRPA is realized with each photocatalytic material. The most common method reported in literature which evaluates photocatalytic activity at equal catalyst concentration may lead to inconclusive results since each material may display significantly different optical properties. This result was confirmed in this study which showed that the modification of commercial TiO_2 catalyst with alcohols with different chain lengths produces materials with significantly different photon absorption properties. The catalyst activity and resistance to deactivation was affected by the deposition of carbon onto the surface of the catalyst as shown in the FTIR results. Overall the catalyst N,C—TiO_2/NH_4OH, 2-butanol was the most active.

Acknowledgments

This work has been supported by the Polish Ministry of Science and Higher Education as a scientific project. Prof. Morawski thanks Prof. Barbara Grzmil from West Pomaranian Univeristy of Technology for the XRD analysis and Dr Dariusz Moszyński also from West Pomaranian Univeristy of Technology for the XPS analysis. G. Li Puma is grateful to NATO (grant CBP.EAP.SFPP 982835) for funding the studies on catalyst activity and kinetic analysis. The authors are grateful to the EU Commission for sponsoring a six months visit of Diana Dolat to the United Kingdom under the ERASMUS mobility programme.

Appendix A. Supplementary data

Supplementary data associated with this article can be found, in the online version, at doi:10.1016/j.apcatb.2011.12.007.

References

[1] J. Zeng, H. Wang, Y. Zhang, M.K. Zhu, H. Yan, J. Phys. Chem. C 111 (2007) 11879–11887.
[2] J. Grzechulska-Damszel, A.W. Morawski, Asia Pac. J. Chem. Eng. 4 (2009) 239–245.
[3] N.G. Chorianopoulos, D.S. Tsoukleris, E.Z. Panagou, P. Falaras, G.-J.E. Nychas, Food Microbiol. 28 (2011) 164–170.
[4] P. Pichat, Appl. Catal. B 99 (2010) 428–434.
[5] M. Norouzi, L. Maleknia, Asian J. Chem. 22 (2010) 5930–5936.
[6] H.A. Foster, D.W. Sheel, P. Sheel, P. Evans, S. Varghese, N. Rutschke, H.M. Yates, J. Photochem. Photobiol. A: Chem. 216 (2010) 283–289.
[7] N.A. Jamalluddin, A.Z. Abdullah, Ultrason. Sonochem. 18 (2011) 669–678.
[8] V. Iliev, D. Tomova, S. Rakovsky, A. Eliyas, G.L. Puma, J. Mol. Catal. A: Chem. 327 (2010) 51–57.
[9] M. Janus, E. Kusiak, A.W. Morawski, Catal. Lett. 131 (2009) 506–511.
[10] C. Cantau, T. Pigot, J.-C. Dupin, S. Lacombe, J. Photochem. Photobiol. A: Chem. 216 (2010) 201–208.
[11] P. Calza, E. Pelizzetti, K. Mogyorósi, R. Kun, I. Dékány, Appl. Catal. B: Environ. 72 (2007) 314–321.
[12] L. Korösi, A. Oszkó, G. Galbács, A. Richardt, V. Zöllmer, I. Dékány, Appl. Catal. B: Environ. 77 (2007) 175–183.
[13] H. Choi, M.G. Antoniou, M. Pelaez, A.A. De La Cruz, J.A. Shoemaker, D.D. Dionysiou, Environ. Sci. Technol. 41 (2007) 7530–7535.
[14] M. Pelaez, P. Falaras, V. Likodimos, A.G. Kontos, A.A. de la Cruz, K. O'shea, D.D. Dionysiou, Appl. Catal. B: Environ. 99 (2010) 378–387.
[15] R. Asahi, T. Morikawa, T. Ohwaki, K. Aoki, Y. Taga, Science 293 (2001) 269–271.
[16] N. Serpone, J. Phys. Chem. B 110 (2006) 24287–24293.
[17] S. Yin, M. Komatsu, Q. Zhang, F. Saito, T. Sato, J. Mater. Sci. 42 (2007) 2399–2404.
[18] D. Chen, Z. Jiang, J. Geng, Q. Wang, D. Yang, Ind. Eng. Chem. Res. 46 (2007) 2741–2746.
[19] D. Noguchi, Y. Kawamata, T. Nagatomo, J. Electrochem. Soc. 152 (2005) 124–129.
[20] Y. Cong, F. Chen, J. Zhang, M. Anpo, Chem. Lett. 35 (2006) 800–801.
[21] C. Yu, J.C. Yu, Catal. Lett. 129 (2009) 462–470.
[22] K.-R. Wu, C.-H. Hung, Appl. Surf. Sci. 256 (2009) 1595–1603.
[23] S. Zhang, L. Song, Catal. Commun. 10 (2009) 1725–1729.
[24] X. Yang, C. Cao, L. Erickson, K. Hohn, R. Maghirang, K. Klabunde, J. Catal. 260 (2008) 128–133.
[25] Y.-H. Tseng, C.-S. Kuo, C.-H. Huang, Y.-Y. Li, Z. Phys. Chem. 224 (2010) 843–856.
[26] X. Wang, T.-T. Lim, Appl. Catal. B: Environ. 100 (2010) 355–364.
[27] C.M. Liu, X.P. Li, X.T. Zu, Chin. J. Phys. 47 (2009) 207–214.
[28] N.N. Binitha, Z. Yaakob, P.P. Silija, M.R. Resmi, P.V. Suraja, Synergistic effect of cobalt on nitrogen and carbon doped anatase titania for photodegradation under visible light, in: Technical Proceedings of the 2010 NSTI Nanotechnology Conference and Expo, NSTI-Nanotech 2010, vol.1, 2010, pp. 464–468.
[29] M. Janus, A.W. Morawski, Appl. Catal. B 75 (2007) 118–123.
[30] M. Janus, M. Toyoda, M. Inagaki, B. Tryba, A.W. Morawski, J. Adv. Oxid. Technol. 10 (2007) 260–266.
[31] A. Gora, B. Toepfer, V. Puddu, G.L. Puma, Appl. Catal. B 65 (2006) 1–10.
[32] P. Kubelka, J. Opt. Soc. Am. 38 (1948) 448–457.
[33] A.B. Murphy, Sol. Energy Mater. Sol. Cells 91 (2007) 1326–1337.
[34] A.B. Murphy, J. Phys. D: Appl. Phys. 39 (2006) 3571–3581.
[35] V. Nadtochenko, N. Denisov, A. Gorenberg, Y. Kozlov, P. Chubukov, J.A. Rengifo, C. Pulgarin, J. Kiwi, Appl. Catal. B 91 (2009) 460–469.
[36] L. Pramatarova, E. Pecheva, R. Presker, M.T. Pham, M.F. Maitz, M. Stutzmann, Eur. Cells Mater. 9 (2005) 9–12.
[37] C. Randorn, S. Wongnawa, P. Boonsin, Sci. Asia 30 (2004) 149–156.

[38] M. Janus, E. Kusiak, J. Choina, J. Ziebro, A.W. Morawski, Desalination 249 (2009) 359–363.
[39] M. Janus, J. Choina, A.W. Morawski, J. Hazard. Mater. 166 (2009) 1–5.
[40] J. Augustynski, Electrochim. Acta 38 (1993) 43–46.
[41] A. Sclafani, J.M. Herrmann, J. Phys. Chem. 100 (1996) 13655–13661.
[42] Y. Cong, J. Zhang, F. Chen, M. Anpo, J. Phys. Chem. C 111 (2007) 6976–6982.
[43] B. Wawrzyniak, A.W. Morawski, Appl. Catal. B 62 (2006) 150–158.
[44] M.L. Satuf, R.J. Brandi, A.E. Cassano, O.M. Alfano, Appl. Catal. B 82 (2008) 37–49.
[45] C. Arancibia-Bulnes, A. Jimenez, C. Estrada, in: H.I. de Lasa, B.S. Rosales (Eds.), Advances in Chemical Engineering, Elsevier, 2009, p. 185.
[46] Y.U. Ahn, E.J. Kim, H.T. Kim, S.H. Hahn, Mater. Lett. 57 (2003) 4660–4666.
[47] X. Chen, S.S. Mao, Chem. Rev. 107 (2007) 2891–2959.
[48] S. Sério, M.E. Melo Jorge, M.J.P. Maneira, Y. Nunes, Mater. Chem. Phys. 126 (2011) 73–81.
[49] R.F.P. Nogueira, J.R. Guimarães, Water Res. 34 (2000) 895–901.
[50] M. Janus, E. Kusiak, J. Choina, A.W. Morawski, Catal. Lett. 131 (2009) 606–611.
[51] M. Addamo, V. Augugliaro, M. Bellardita, A. Di Paola, V. Loddo, G. Palmisano, L. Palmisano, S. Yurdakal, Catal. Lett. 126 (2008) 58–62.
[52] S. Yurdakal, G. Palmisano, V. Loddo, O. Alagoz, V. Augugliaro, L. Palmisano, Green Chem. 11 (2009) 510–516.
[53] J. Colina-Marquez, F. Machuca-Martinez, G.L. Puma, Environ. Sci. Technol. 44 (2010) 5112–5120.